Supplementary data

Whole Exome Sequencing and Analyses

For patient 1, exome capture was performed on 3 μg of genomic DNA using the Agilent SureSelect liquid-phase hybridization capture system (Human All Exons kit 51Mb, V5). Single-end sequencing was performed on an Illumina Genome Analyzer IIx (Illumina) generating 72-base reads. Sequence data were analyzed by the Bioinformatic platform and visualized via the interface created by the Bioinformatic platform (Paris Descartes University, Paris). For patient 3, clinical WES was performed at Ambry Genetics, CA USA. For patient 4 and patient 5, WES was performed as a quartet including two affected siblings and both parents. Genomic DNA was purified from fresh whole blood using the Gentra Puregene Kit (Qiagen Sciences, Germantown, MD). WES was performed using the Agilent SureSelect Human All Exon 50Mb Kit (Agilent Technologies, Santa Clara, CA) and paired end 100 bp reads using the Illumina HiSeq2000 platform (Illumina, Inc. San Diego, CA). Only the variants in *DEGS1* segregated correctly with the phenotype in this family and this gene was submitted to GeneMatcher (1). For patient 6, whole-exome sequencing (WES) at Centro Nacional de Análisis Genómico in Barcelona (CNAG) was performed on exon targets isolated by capture using the SeqCap EZ Human Exome Kit v3·0 (Roche Nimblegen, USA) with 100-bp paired-end read sequences generated on a HiSeq2000 (Illumina, Inc. USA) in the CNAG. The sequencing methodology and variant interpretation protocol was identified through the Genome Analysis Tool Kit (GATK) pipeline (2). Sequence processing was carried out with BWA aligner (3), the Genome Analysis Toolkit (GATK) (2), SAMtools (4) and Picard Tools. For patients 7, 9 and 10, WES was performed by IntegraGen SA (Evry, France) as previously described (5), and WES data analysis was performed using an in-house implemented pipeline (6). For patient 13 and 18, in solution exome capture was performed using the SureSelect Human All Exome 50 Mb Kit (Agilent Technologies, USA) with 100-bp paired-end read sequences generated on a HiSeq2000 (Illumina, Inc. USA. Sequences were aligned to hg19 and variants identified through the GATK pipeline (2). Variations were annotated with in-house software and the SeattleSeq server (7). For patient 14, WES was performed at McGill University and Genome Quebec Innovation Centre (Montreal), Exome target enrichment was performed with the Agilent SureSelect 50 Mb (V3) All Exon Kit; samples were sequenced on the Illumina HiSeq 2000 platform, multiplexing three

samples per lane. After removal of duplicate reads, the mean coverage of coding sequence regions ranged from ×70 to ×200. Alignment and variant annotation were performed by the FORGE informatics team, using comparable analytical pipelines with publicly available tools and custom scripts (8). For patients 15 and 16, WES was conducted clinically through Baylor Genetics, Houston, Texas. For massively parallel sequencing, the postcapture library DNA is subjected to sequence analysis on Illumina HiSeq platform for 100 bp paired-end reads. Data analysis and interpretation by Mercury: The output data from Illumina HiSeq are converted from bcl file to FastQ file by Illumina CASAVA 1.8 software (Illumina, San Diego, California, USA), and mapped by BWA program to the reference haploid human genome sequence (Genome Reference Consortium human genome build 37, human genome 19). For patient 17, Capture for WES was performed with NimbleGen SeqCap EZ Exome Library v1.0 kit (Roche, Indianapolis, IN). Captured regions were sequenced with Illumina HiSeq2000 instruments. For patient 19, Capture for WES was performed with the SureSelectXT Human All Exon v5 kit (Agilent). Sequencing was performed using the Illumina HiSeq2500 (Otogenetics Corporation, Atlanta, GA USA) to generate paired-end reads of 125 nucleotides with an average coverage of 30X. All variants were prioritized by allele frequency, conservation, and predicted effect on protein function, and were tested for segregation with disease.

Cell culture and treatments

Primary human fibroblasts were cultivated as described (9). Skin biopsies to prepare control and DEGS1 patient's fibroblasts were collected according to the institutional guidelines for sampling, including informed consent from the subjects involved or their representatives. Unless otherwise stated, the experiments were performed with cells at 80% confluence. Fingolimod, FTY720 (Selleckchem, USA) was dissolved in DMSO and kept at -80 °C until used. C18 Dihydroceramide (d18:0/18:0) was purchased from Avanti Polar Lipids (860627) and was brought up in ethanol/dodecane 49:1 (v/v) solution. After solubilization, the DhCer solution was kept at 37 °C until addition to reaction tube.

RNA extraction and quantitative real-time PCR

Total RNA was extracted using RNeasy Kit (Qiagen). To quantify mRNA levels, 1 μg of RNA was transcribed into cDNA using Superscript IV reverse transcription reagents

in a final volume of 25 µl (Invitrogen, Thermo Fisher Scientific Inc., Waltham, MA, USA). 1:75 dilution of cDNA was used to measure mRNA levels. TaqMan real-time PCR was performed in the Lightcycler 384 sequence detection system (Roche) using the TaqMan Universal PCR master mix and the standardized primers (mouse *Degs1* and human *DEGS1* were Mm00492146_m1, Hs00186447_m1, respectively), (mouse *Degs2* and human *DEGS2* were Mm00510313_m1, Hs01380343_m1, respectively) (Thermo Fisher Scientific Inc., Waltham, MA, USA). Expression of the gene of interest was normalized to that of the reference control (mouse *Rplp0* and human *RPLP0* were Mm01974474_gH, Hs9999902_m1, respectively). Each sample was run in triplicate, and the mean value of the triplicate was used to calculate the RNA expression using the comparative ($2^{-\Delta Ct}$) method, according to the manufacturer's instructions.

Evaluation of intracellular radical oxygen species

Intracellular radical oxygen species levels were estimated using the ROS-sensitive H_2DCFDA probe (Invitrogen, Thermo Fisher Scientific Inc., Waltham, MA, USA) as described (10). Following incubation with 10 µM H_2DCFDA for 30 min at 37 °C, cells were washed twice with PBS and lysate with 1% Triton™. The fluorescence of H_2DCFDA stained cells was measured with a spectrofluorimeter (excitation wavelength 493 nm, emission wavelength 527 nm).

Supplementary figures

Supplementary Figure 1. **Pedigrees and sequencing chromatograms of families affected by *DEGS1* variants.** Variants in probands verified by Sanger sequencing are indicated by arrows. Sanger sequencing could not be performed for individuals where genetic material was not available (n.a.).

Supplementary Figure 2. Sequential Brain MRIs patients 4 and 10. (A) Patient 4 (top rows) MRI at 2 years of age shows delayed myelination, thalamic FLAIR hyperintensities in bilateral anterior and lateral thalami and in pulvinar (white arrows). The sagittal T1 image shows thinning of CC (black arrow). (B) A follow -up MRI at age 4 shows mildly improved myelination in centrum semiovale. However, there is hypointense T1 signal in the occipital deep white matter white matter, suggesting that demyelination is superimposed on hypomyelination. Sagittal T1 image shows progressive atrophy of CC and subtle cerebellar atrophy. Patient 10 (low rows): (C) Initial MRI at age 2 showed severely abnormal confluent T2 signal involving the

centrum semiovale and posterior periventricular WM. Hyperintensities in the thalami were seen in the same distribution as that in patient 4. The T1-weighted images show normal signal in most areas but again hypointense signal in the occipital deep WM, suggesting demyelination superimposed on hypomyelination. (D) A follow-up study at age 12 shows a severe cerebral atrophy predominant in the fronto-parietal regions with enlargement of the Sylvian fissures. The cerebellar atrophy has progressed, with thinning of CC (black arrow) and atrophied thalami (white arrow).

Supplementary Figure 3. Relative gene expression.

(A) *DEGS1* expression measured by quantitative RT-PCR in different CNS tissues of control human children and adults (n=2). (B) *Degs1* and *Degs2* expression measured by quantitative RT-PCR in several tissues from 4-month-old mice (n=3). Gene expression normalized relative to *Rplp0*. (C) *DEGS1* and *DEGS2* expression measured by quantitative RT-PCR in human control (n=5) and patient fibroblasts (P4, P7, P9). Gene expression normalized relative to *RPLP0*. Experiments with fibroblasts were performed in triplicates. Data are shown as the means ± SD; * $p<0{\cdot}05$; ** $p<0{\cdot}01$; *** $p<0{\cdot}001$ after one-way ANOVA test followed by Tukey's post hoc test.

Supplementary Figure 4. **Localization of *degs1* transcripts in *Danio rerio* larvae and *degs1* knockdown using splice blocker morpholino**

In situ hybridization for *degs1* either of whole-mount larvae (A), or of sections (B-D) of 5 dpf larvae. (A) Whole-mount embryo *in situ* hybridization presented in lateral view (n=10) (B-D). Scale bar: 10 µm. Transverse histological sections at different levels along the antero-posterior axis: head, hindbrain and spinal cord (n=5). Note that hybridization signal is reinforced in (B) TeO, DT, PT, and E in head, (C) MO and CeP in hindbrain and (D) spinal cord. (E-F) Immunofluorescence localization of GFP in histological sections of zebrafish larvae *Tg[mbp:egfp]* of (C-D) respectively. Scale bar: 10 µm. Note that *degs1* expression overlaps with GFP in the hindbrain and spinal cord. CNS, central nervous system; B, brain; DT, dorsal thalamus; E, eye; PT, posterior tuberculum; TeO, tectum opticum; MO, medulla oblongata; CeP, cerebellar plate; HB, hindbrain; SC, spinal cord. (G) Scheme depicting the structure of zebrafish *degs1* gene depicting the exons in black solid boxes and untranslated regions as white boxes. Vertical arrow indicates the splice-blocking (sb) morpholino (MO) target site at the exon 2–intron 2 (e2i2) boundary. Horizontal arrows indicate the position of the primers

used to genotype. (H) Agarose gel showing the aberrant splicing products induced by the morpholinos, as detected by RT–PCRs (right) at 3 dpf (n=10 by condition). Note that the morphant embryos display aberrant transcripts with the inclusion of intron 2 (+97 bp). (I) Chromatograms of PCR product (bottom) demonstrate that the e2i2 sb MO induces inclusion of the intron.

Supplementary tables

Table 1. Molecular data and individual variant description from all 19 patients from 13 unrelated families

[a] The reference genome used for bioinformatic predictions is GRCh37/hg19. [b] HGVSc/HGVSp: coding DNA/protein variant described according to the nomenclature established by the Human Genome Variation Society. [c] SIFT (sift); D: Deleterious (sift<=0.05); T: tolerated (sift>0.05). [d] PolyPhen-2 HumDiv: PolyPhen-2 Human Diversity; D: Probably damaging (>=0.957), P: possibly damaging (0.453<=pp2_hdiv<=0.956); B: benign (pp2_hdiv<=0.452). [e] PolyPhen-2 HumVar: PolyPhen-2 Human Variation; D: Probably damaging (>=0.909), P: possibly damaging (0.447<=pp2_hdiv<=0.909); B: benign (pp2_hdiv<=0.446). [f] CADD: Combined Annotation Dependent Depletion; higher scores are more deleterious. [g] LRT: likelihood ratio test; D: Deleterious; N: Neutral; U: Unknown. [h] MutationTaster; A" ("disease_causing_automatic"); "D" ("disease_causing"); "N" ("polymorphism"); "P" ("polymorphism_automatic"). [i] MutationAssessor; H: high; M: medium; L: low; N: neutral. H/M means functional and L/N means non-functional.[j] FATHMM: functional Analysis through Hidden Markov models; D: Deleterious; T: Tolerated. [k] PROVEAN: Protein Variation Effect Analyzer: D: Deleterious; N: Neutral. [l] MetaSVM: radial basis function kernel support vector machine; D: Deleterious; T: Tolerated. [m] MetaLR: logistic regression; D: Deleterious; T: Tolerated. [n] M-CAP: Mendelian Clinically Applicable Pathogenicity; D: Deleterious; T: Tolerated. [o] fathmm-MKL: functional Analysis through Hidden Markov models; D: Deleterious; T: Tolerated. [p] VEST3: Variant Effect Scoring Tool; higher scores are more deleterious. [q] REVEL: higher scores are more deleterious. [r] GERP: Genomic Evolutionary Rate Profiling, RS score: “rejected substitutions” score; higher scores are more deleterious. [s] PhyloP100way_vertebrate: PhyloP basewise conservation score derived from Multiz alignment of 100 vertebrate species; higher scores are more deleterious. [t] PhyloP20way mammalian: PhyloP basewise conservation score derived from Multiz alignment of 20

mammals; PhyloP scores measure evolutionary conservation at individual alignment sites; higher scores are more deleterious. [u] SiPhy_29way_logOdds: SIte-specific PHYlogenetic analysis; based on a high-resolution map of evolutionary constraint in the human genome based on 29 eutherian mammals; higher scores are more deleterious. [v] Interpro domain: interPro predicted domains. [w] Frequence Databases queried: 1000 Genomes data (version 2015 Aug, from Annovar), the NHLBI GO Exome Sequencing Project (ESP) data (ESP6500SI-V2, from Annovar); the Exome Aggregation Consortium (ExAC) (Cambridge, MA (URL: http://exac.broadinstitute.org) [accessed on January 2018]), the Genome Aggregation Database (GnomAD) (URL: http://gnomad.broadinstitute.org/) [last accessed on June 2018].

Table 2. LC-ESI MS/MS analysis of N-acyl chain Cer and DhCer species distribution in zebrafish larvae of MO-control and MO-DEGS1. Experiments were performed at 5dpf +/- FTY720 (1 ng/µl) treatment. The % of individual Cer and DhCer were calculated with respect to the total Cer, DhCer respectively. Values are mean ± SD (% of total lipids analysed; n = 4) * $p<0.05$; ** $p<0.01$; *** $p<0.001$ after two-way ANOVA test followed by Tukey's post hoc test. a, indicates significant change in MO-DEGS1 from MO-control; b, indicates significant change in MO-DEGS1 after FTY720; in addition these significant correction with treatment are shadowed.

Table 3. List of primers used for Sanger validation

References

1. Sobreira, N., Schiettecatte, F., Valle, D., and Hamosh, A. 2015. GeneMatcher: a matching tool for connecting investigators with an interest in the same gene. *Hum Mutat* 36:928-930.
2. McKenna, A., Hanna, M., Banks, E., Sivachenko, A., Cibulskis, K., Kernytsky, A., Garimella, K., Altshuler, D., Gabriel, S., Daly, M., et al. 2010. The Genome Analysis Toolkit: a MapReduce framework for analyzing next-generation DNA sequencing data. *Genome Res* 20:1297-1303.
3. Li, H., and Durbin, R. 2010. Fast and accurate long-read alignment with Burrows-Wheeler transform. *Bioinformatics* 26:589-595.
4. Li, H., Handsaker, B., Wysoker, A., Fennell, T., Ruan, J., Homer, N., Marth, G., Abecasis, G., and Durbin, R. 2009. The Sequence Alignment/Map format and SAMtools. *Bioinformatics* 25:2078-2079.
5. Guichard, C., Amaddeo, G., Imbeaud, S., Ladeiro, Y., Pelletier, L., Maad, I.B., Calderaro, J., Bioulac-Sage, P., Letexier, M., Degos, F., et al. 2012. Integrated analysis of somatic mutations and focal copy-number changes identifies key genes and pathways in hepatocellular carcinoma. *Nat Genet* 44:694-698.
6. Vanderver, A., Simons, C., Helman, G., Crawford, J., Wolf, N.I., Bernard, G., Pizzino, A., Schmidt, J.L., Takanohashi, A., Miller, D., et al. 2016. Whole

exome sequencing in patients with white matter abnormalities. *Ann Neurol* 79:1031-1037.

7. Dixon-Salazar, T.J., Silhavy, J.L., Udpa, N., Schroth, J., Bielas, S., Schaffer, A.E., Olvera, J., Bafna, V., Zaki, M.S., Abdel-Salam, G.H., et al. 2012. Exome sequencing can improve diagnosis and alter patient management. *Sci Transl Med* 4:138ra178.
8. Beaulieu, C.L., Majewski, J., Schwartzentruber, J., Samuels, M.E., Fernandez, B.A., Bernier, F.P., Brudno, M., Knoppers, B., Marcadier, J., Dyment, D., et al. 2014. FORGE Canada Consortium: outcomes of a 2-year national rare-disease gene-discovery project. *Am J Hum Genet* 94:809-817.
9. Morato, L., Ruiz, M., Boada, J., Calingasan, N.Y., Galino, J., Guilera, C., Jove, M., Naudi, A., Ferrer, I., Pamplona, R., et al. 2015. Activation of sirtuin 1 as therapy for the peroxisomal disease adrenoleukodystrophy. *Cell Death Differ* 22:1742-1753.
10. Lopez-Erauskin, J., Galino, J., Ruiz, M., Cuezva, J.M., Fabregat, I., Cacabelos, D., Boada, J., Martinez, J., Ferrer, I., Pamplona, R., et al. 2013. Impaired mitochondrial oxidative phosphorylation in the peroxisomal disease X-linked adrenoleukodystrophy. *Hum Mol Genet* 22:3296-3305.

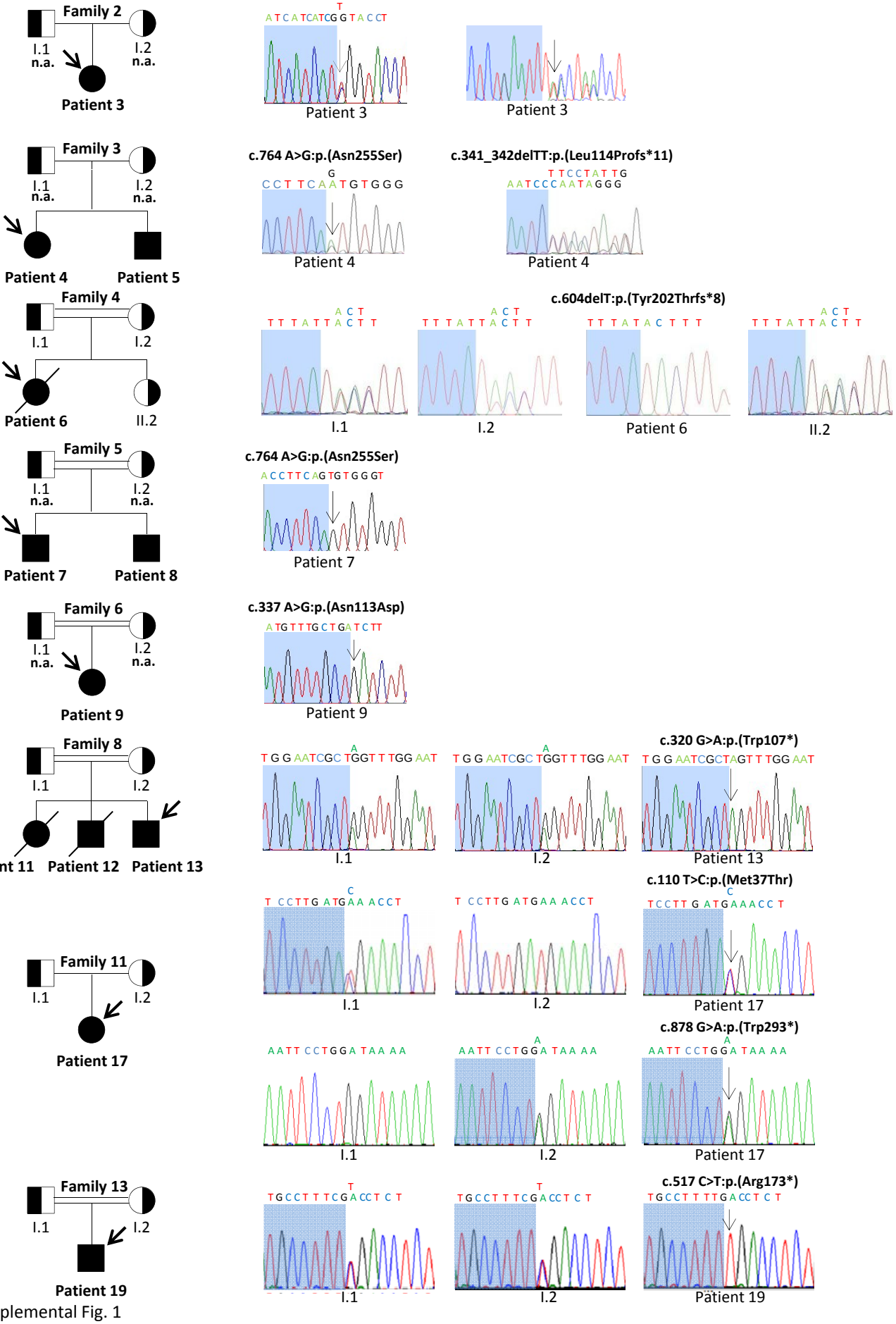

Supplemental Fig. 1

A Patient 4 (2y)

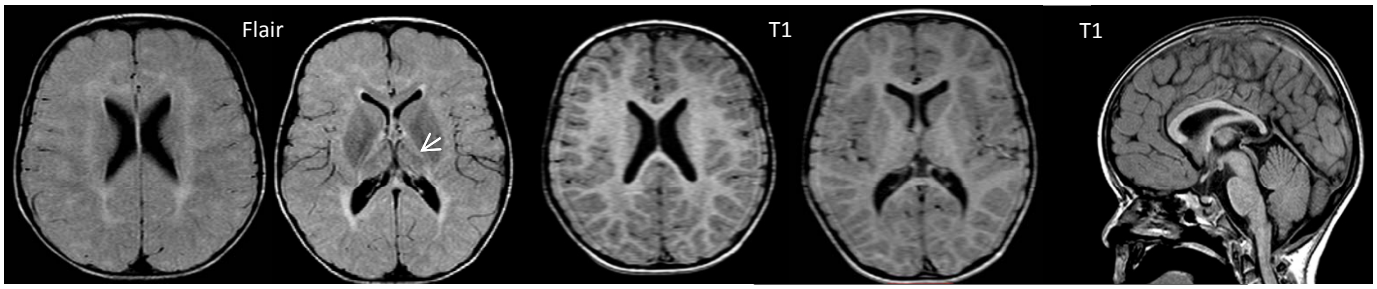

B Patient 4 (4y)

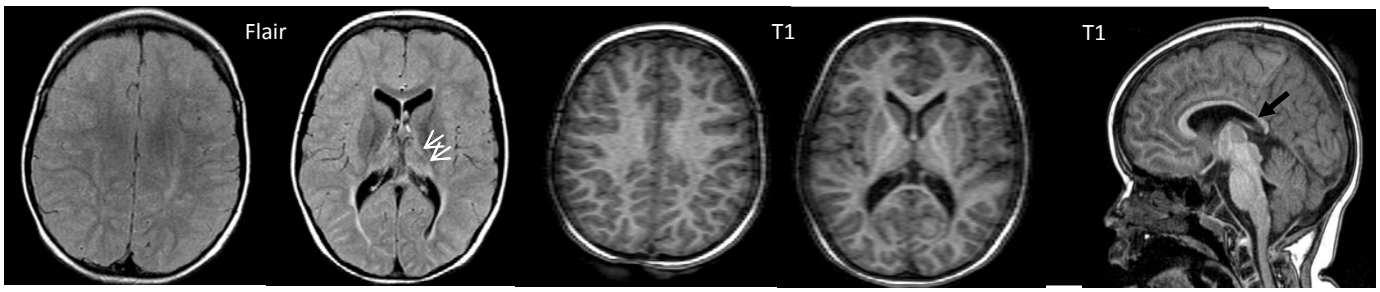

C Patient 10 (2y)

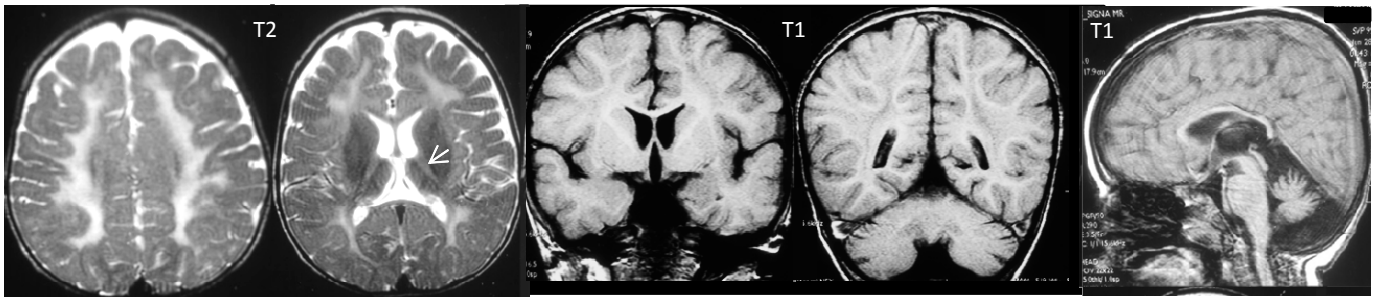

D Patient 10 (12y)

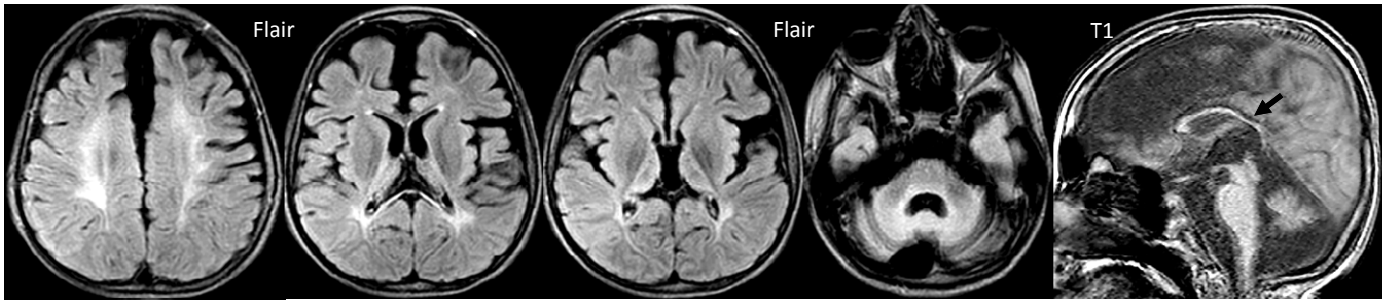

Supplemental Fig. 2

A

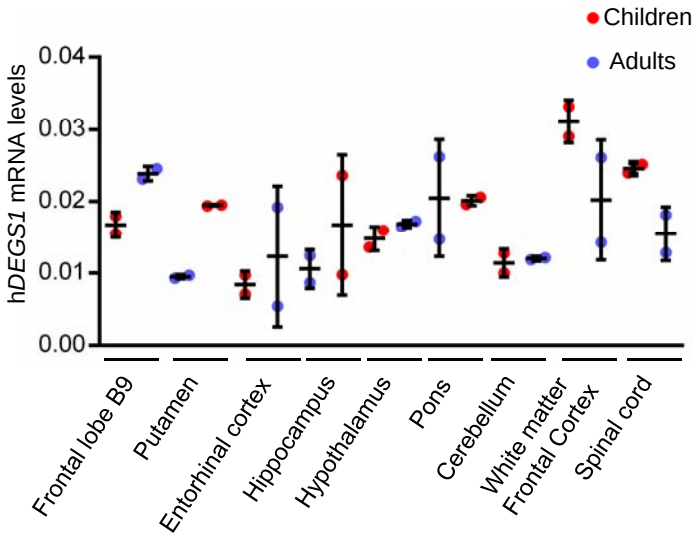

B

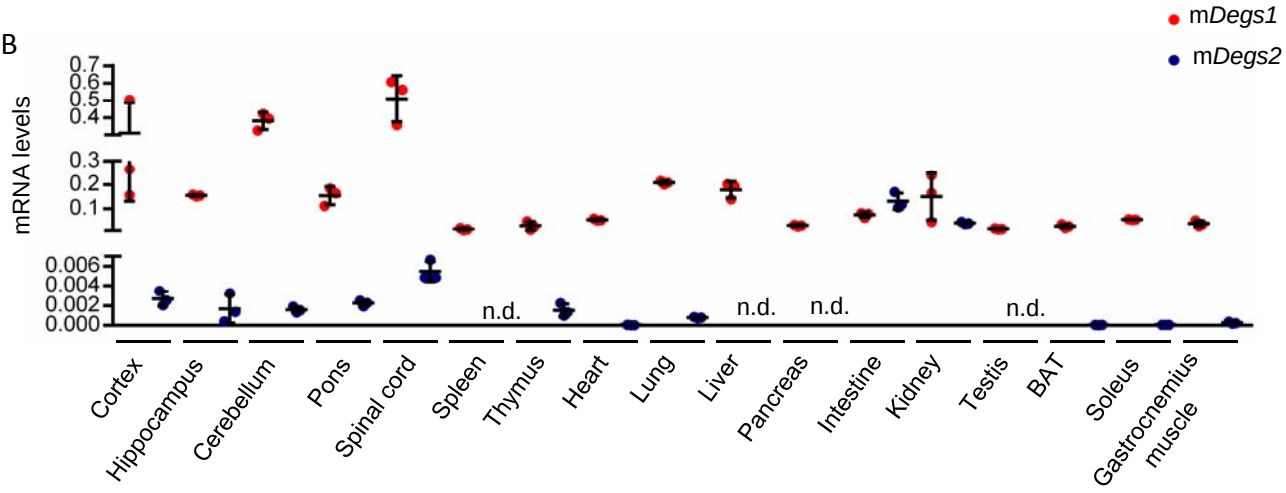

C

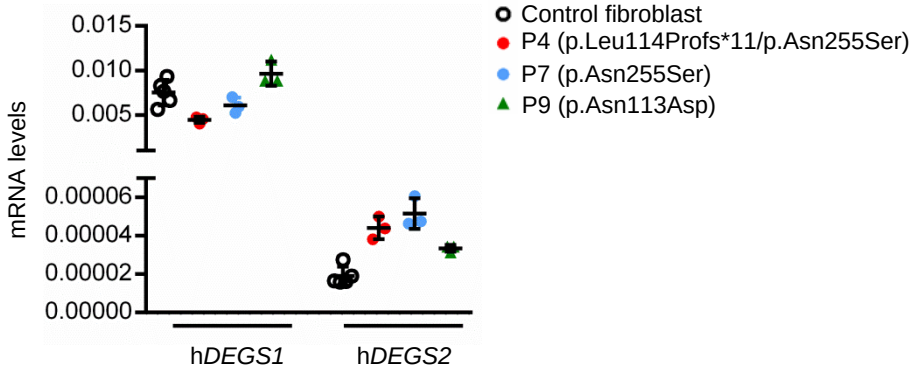

Supplemental Fig. 3

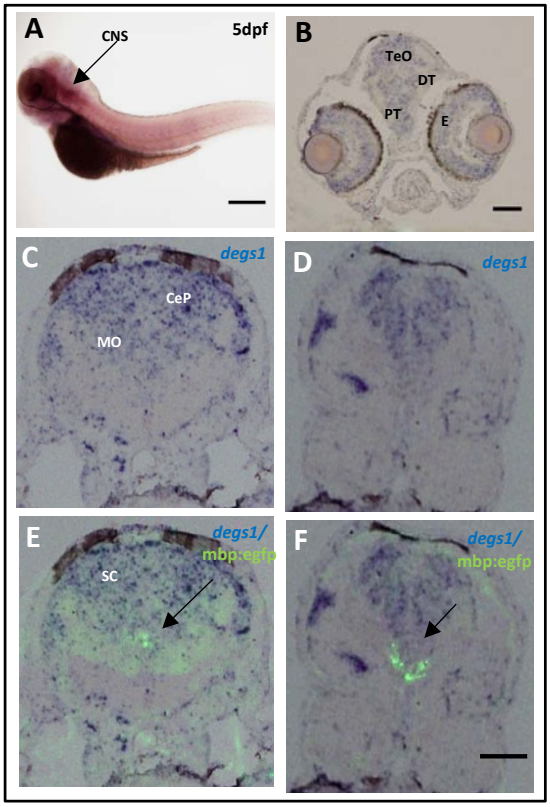

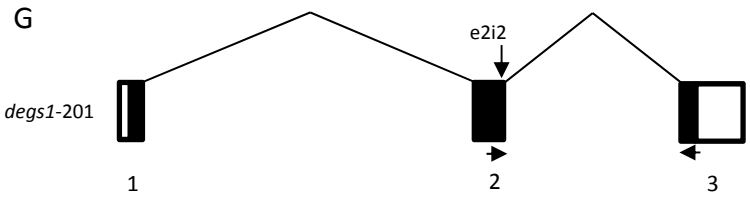

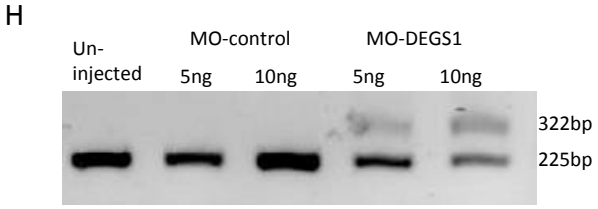

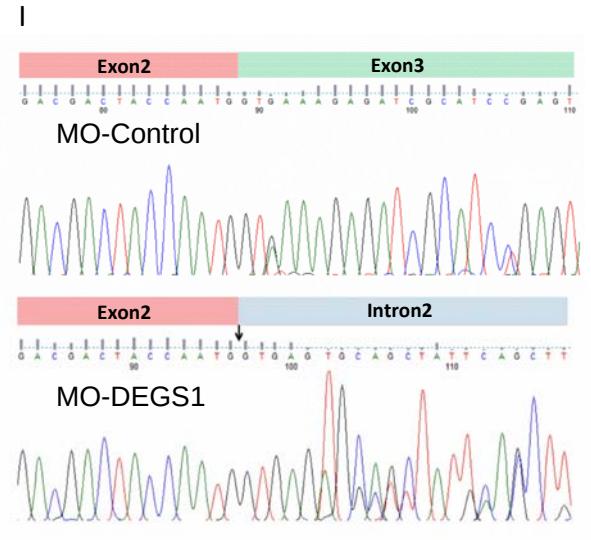

Supplemental Fig. 4

Variants	Chromosomal position of the variant [a]	HGVSc [b] (exon)	HGVSp [b] (amino acids)	rs	Exonic variant function	SIFT (score) [c]	Polyphen2 HDIV (score) [d]
1	Chr1(GRCh37):g.224377306T>C	NM_003676.3:c.110T>C (exon 2/3)	p.(Met37Thr)	.	nonsynonymous SNV	D (0.012)	D (0.984)
2	Chr1(GRCh37):g.224377516G>A	NM_003676.3:c.320G>A (exon 2/3)	p.(Trp107*)	.	stopgain	.	.
3	Chr1(GRCh37):g.224377533A>G	NM_003676.3:c.337A>G (exon 2/3)	p.(Asn113Asp)	.	nonsynonymous SNV	D (0.002)	D (1.0)
4	Chr1(GRCh37):g:224377537_224377538delTT	NM_003676.3:c.341_342delTT (exon 2/3)	p.(Leu114Profs*11)	.	frameshift deletion	.	.
5	Chr1(GRCh37):g.224377591A>G	NM_003676.3: c.395A>G (exon 2/3)	p.(His132Arg)	.	nonsynonymous SNV	D (0.0)	D (1.0)
6	Chr1(GRCh37):g.224377593C>T	NM_003676.3:c.397C>T (exon 2/3)	p.(Arg133Trp)	.	nonsynonymous SNV	D (0.0)	D (1.0)
7	Chr1(GRCh37):g. 224377713 C>T	NM_003676.3: c.517C>T (exon 2/3)	p.(Arg173*)	.	stopgain	.	.
8	Chr1(GRCh37):g.224377761A>G	NM_003676.3:c.565A>G (exon 2/3)	p.(Asn189Asp)	rs771864122	nonsynonymous SNV	D (0.002)	D (0.999)
9	Chr1(GRCh37):g.224377800delT	NM_003676.3:c.604delT (exon 2/3)	p.(Tyr202Thrfs*8)	.	frameshift deletion	.	.
10	Chr1(GRCh37):g.224377948dupT	NM_003676.3: c752dupT (exon 2/3)	p.(Leu251Phefs*10)	.	frameshift insertion	.	.
11	Chr1(GRCh37):g.224377960A>G	NM_003676.3:c.764A>G (exon 2/3)	p.(Asn255Ser)	rs768180196	nonsynonymous SNV	D (0.032)	B (0.241)
12	Chr1(GRCh37):g.224380060_224380063delTGAC	NM_003676.3:c.852_855del (exon 3/3)	p.(Tyr284*)	.	stopgain	.	.
13	Chr1(GRCh37):g.224380086G>A	NM_003676.3: c.878G>A (exon 3/3)	p.(Trp293*)	.	stopgain	.	.

Variants	Polyphen2 HVAR (score) [e]	CADD (raw score) [f]	CADD (phred score) [f]	LRT (score) [g]	MutationTaster (score) [h]	MutationAssessor (score) [i]	FATHMM (score) [j]	PROVEAN (score) [k]	MetaSVM (score) [l]	MetaLR (score) [m]	M-CAP (score) [n]	fathmm-MKL coding score [o]
1	D (0.917)	4.723	24.6	D (0.00)	D (1.00)	M (2.9)	T (0.85)	D (-4.49)	T (-0.637)	T (0.269)	D (0.041)	D (0.990)
2	.	10.813	36	D (0.00)	A (1.00)	.	.	.	.	.	.	D (0.939)
3	D (0.999)	5.856	27.3	D (0.00)	D (1.00)	M (2.88)	T (2.33)	D (-4.53)	T (-0.873)	T (0.146)	D (0.032)	D (0.991)
4	.	.	.	.	.	.	.	.	.	.	.	.
5	D (1.0)	4.921	25.0	D (0.00)	D (1.00)	H (3.98)	D (-3.04)	D (-7.91)	D (1.076)	D (0.921)	D (0.244)	D (0.991)
6	D (0.995)	6.967	33	D (0.00)	D (1.00)	H (3.59)	T (2.14)	D (-7.67)	T (-0.438)	T (0.212)	D (0.121)	D (0.974)
7	.	11,646	37	D (0.00)	A (1.00)	.	.	.	.	.	.	D (0.929)
8	D (0.998)	4.611	24.4	D (0.00)	D (1.00)	H (4.005)	T (2.31)	D (-4.62)	T (-0.399)	T (0.211)	D (0.035)	D (0.992)
9	.	.	.	.	.	.	.	.	.	.	.	.
10	.	.	.	.	.	.	.	.	.	.	.	.
11	P (0.571)	4.337	24.0	D (0.00)	D (1.00)	M (3.285)	T (1.9)	D (-4.62)	T (-0.701)	T (0.199)	D (0.052)	D (0.990)
12	.	.	.	.	.	.	.	.	.	.	.	.
13	.	13.658	43	D (0.00)	A (1.00)	.	.	.	.	.	.	D (0.993)

Variants	VEST3 (score) [p]	REVEL [q]	GERP++ RS [r]	phyloP100way_vertebrate [s]	phyloP20way_mammalian [t]	SiPhy_29way_logOdds [u]	Interpro domain [v]	1000G_ALL [w]	ExAC_ALL [w]	P6500siv2_AL	nomAD_ALL [v]
1	0.861	0.512	5.45	8.010	1.051	15.823	Sphingolipid delta4-desaturase / Fatty acid desaturase domain	.	.	.	.
2	.	.	5.72	3.145	1.038	20.242	Fatty acid desaturase domain	.	.	.	4.061e-06
3	0.531	0.466	5.72	9.317	1.187	16.297	Fatty acid desaturase domain	.	.	.	.
4	.	.	.	.	.	.	Fatty acid desaturase domain	.	.	.	.
5	0.993	0.957	6.02	9.317	1.187	16.543	Fatty acid desaturase domain	.	.	.	.
6	0.927	0.558	5.09	6.181	0.927	16.490	Fatty acid desaturase domain	.	.	.	4.061e-06
7	.	.	4,98	3,34	0,014	14,094	Fatty acid desaturase domain	.	.	.	.
8	0.639	0.550	6.02	9.317	1.187	16.543	Fatty acid desaturase domain	.	8.237e-06	.	4.061e-06
9	.	.	.	.	.	.	Fatty acid desaturase domain	.	.	.	.
10	.	.	.	.	.	.	Fatty acid desaturase domain	.	.	.	9.877e-06
11	0.434	0.442	5.8	9.317	0.233	16.144	Fatty acid desaturase domain	.	5.445e-05	.	5.859e-05
12	.	.	.	.	.	.	Fatty acid desaturase domain	.	.	.	.
13	.	.	5.85	9.602	0.953	20.177	Fatty acid desaturase domain	.	.	.	.

Supplemental Table 1.

a The reference genome used for bioinformatic predictions is GRCh37/hg19.
b HGVSc/HGVSp: coding DNA/protein variant described according to the nomenclature established by the Human Genome Variation Society.
c SIFT (sift); D: Deleterious (sift<=0.05); T: tolerated (sift>0.05)
d PolyPhen-2 HumDiv: PolyPhen-2 Human Diversity; D: Probably damaging (>=0.957), P: possibly damaging (0.453<=pp2_hdiv<=0.956); B: benign (pp2_hdiv<=0.452)
e PolyPhen-2 HumVar: PolyPhen-2 Human Variation; D: Probably damaging (>=0.909), P: possibly damaging (0.447<=pp2_hdiv<=0.909); B: benign (pp2_hdiv<=0.446)
f CADD: Combined Annotation Dependent Depletion; higher scores are more deleterious
g LRT: likelihood ratio test; D: Deleterious; N: Neutral; U: Unknown
h MutationTaster; A" ("disease_causing_automatic"); "D" ("disease_causing"); "N" ("polymorphism"); "P" ("polymorphism_automatic")
i MutationAssessor; H: high; M: medium; L: low; N: neutral. H/M means functional and L/N means non-functional
j FATHMM: functional Analysis through Hidden Markov models; D: Deleterious; T: Tolerated
k PROVEAN: Protein Variation Effect Analyzer: D: Deleterious; N: Neutral
l MetaSVM: radial basis function kernel support vector machine; D: Deleterious; T: Tolerated
m MetaLR: logistic regression; D: Deleterious; T: Tolerated
n M-CAP: Mendelian Clinically Applicable Pathogenicity; D: Deleterious; T: Tolerated
o fathmm-MKL: functional Analysis through Hidden Markov models; D: Deleterious; T: Tolerated
p VEST3: Variant Effect Scoring Tool; higher scores are more deleterious.
q REVEL: higher scores are more deleterious.
r GERP: Genomic Evolutionary Rate Profiling, RS score: “rejected substitutions” score; higher scores are more deleterious
s PhyloP100way_vertebrate: PhyloP basewise conservation score derived from Multiz alignment of 100 vertebrate species; higher scores are more deleterious
t PhyloP20way mammalian: PhyloP basewise conservation score derived from Multiz alignment of 20 mammals; PhyloP scores measure evolutionary conservation at individual alignment sites; higher scores are more deleterious
u SiPhy_29way_logOdds: SIte-specific PHYlogenetic analysis; based on a high-resolution map of evolutionary constraint in the human genome based on 29 eutherian mammals; higher scores are more deleterious
v Interpro domain: interPro predicted domains.
w Frequence Databases queried: 1000 Genomes data (version 2015 Aug, from Annovar), the NHLBI GO Exome Sequencing Project (ESP) data (ESP6500SI-V2, from Annovar); the Exome Aggregation Consortium (ExAC) (Cambridge, MA (URL: http://exac.broadinstitute.org) [accessed on January 2018]), the Genome Aggregation Database (gnomAD) (URL: http://gnomad.broadinstitute.org/) [accessed on January 2018]

Supplementary Table S2

N-acyl FA Species	MO-Control				MO-DEGS1			
	Veh		FTY720		Veh		FTY720	
C7:0-Cer	0.083 ± 0.03		0.09 ± 0.017		0.029 ± 0.005 [a*]		0.088 ± 0.009 [b**]	
C8:0-Cer	0.015 ± 0.007		0.022 ± 0.012		0.016 ± 0.009		0.027 ± 0.013	
C10:0-Cer	35.929 ± 12.5		44.244 ± 10.89		3.560 ± 2.954 [a**]		28.761 ± 12.199 [b*]	
C11:0-Cer	0.051 ± 0.02		0.017 ± 0.007		0.023 ± 0.014 [a*]		0.009 ± 0.004	
C12:0-Cer	13.817 ± 5.52		3.601 ± 5.101		15.866 ± 1.003 [a*]		11.482 ± 4.358	
C13:0-Cer	0.052 ± 0.014		0.046 ± 0.018		0.024 ± 0.027 [a*]		0.029 ± 0.011	
C14:0-Cer	0.032 ± 0.016		0.038 ± 0.023		0.077 ± 0.056		0.056 ± 0.030	
C15:0-Cer	0.086 ± 0.068		0.069 ± 0.051		0.092 ± 0.052 [a**]		0.075 ± 0.025	
C16:0-Cer	11.701 ± 2.232		10.125 ± 3.644		25.188 ± 4.494		21.774 ± 2.883	
C17:0-Cer	0.229 ± 0.122		0.173 ± 0.069		0.317 ± 0.201		0.212 ± 0.064	
C18:0-Cer	4.339 ± 2.000		3.512 ± 0.879		2.315 ± 1.232		4.402 ± 1.004	
C20:0-Cer	1.896 ± 0.601		1.826 ± 0.800		2.192 ± 1.158		2.276 ± 0.513	
C21:0-Cer	0.183 ± 0.058		0.160 ± 0.069		0.280 ± 0.092		0.196 ± 0.053	
C22:0-Cer	2.430 ± 0.427		2.228 ± 0.836		4.176 ± 2.133 [a**]		2.817 ± 0.731 [b**]	
C23:0-Cer	0.773 ± 0.160		0.507 ± 0.201		1.599 ± 0.866 [a***]		0.678 ± 0.130 [b***]	
C24:0-Cer	3.554 ± 0.658		2.529 ± 0.880		8.256 ± 1.500 [a***]		3.202 ± 0.798 [b***]	
C25:0-Cer	0.438 ± 0.078		0.320 ± 0.071		1.293 ± 0.328 [a***]		0.288 ± 0.04 [b**]	
C26:0-Cer	2.048 ± 0.611		1.24 ± 0.253		3.889 ± 0.796 [a*]		1.860 ± 0.67 [b***]	
C27:0-Cer	1.382 ± 0.073		0.078 ± 0.111		2.058 ± 0.566		1.328 ± 0.566	
C28:0-Cer	1.595 ± 0.703		0.929 ± 0.143		2.398 ± 0.582		1.485 ± 0.603	
C7:1-Cer	0.014 ± 0.010		0.012 ± 0.007		0.015 ± 0.009		0.007 ± 0.006	
C8:1-Cer	0.033 ± 0.013		0.016 ± 0.007		0.031 ± 0.026		0.016 ± 0.005	
C9:1-Cer	0.012 ± 0.005		0.015 ± 0.011		0.0 ± 0.0		0.002 ± 0.005	
C10:1-Cer	0.038 ± 0.046		0.026 ± 0.011		0.055 ± 0.033		0.028 ± 0.024	
C11:1-Cer	0.025 ± 0.014		0.014 ± 0.012		0.036 ± 0.016		0.008 ± 0.008	
C12:1-Cer	0.019 ± 0.028		0.007 ± 0.012		0.018 ± 0.007		0.006 ± 0.002	
C13:1-Cer	0.010 ± 0.010		0.010 ± 0.001		0.018 ± 0.016		0.019 ± 0.012	
C14:1-Cer	0.016 ± 0.013		0.011 ± 0.007		0.050 ± 0.034		0.030 ± 0.017	
C15:1-Cer	0.078 ± 0.068		0.032 ± 0.007		0.120 ± 0.066		0.074 ± 0.051	
C16:1-Cer	0.057 ± 0.053		0.033 ± 0.015		0.048 ± 0.020		0.035 ± 0.015	
C17:1-Cer	0.012 ± 0.009		0.0006 ± 0.001		0.005 ± 0.008		0.012 ± 0.014	
C18:1-Cer	0.037 ± 0.035		0.021 ± 0.014		0.051 ± 0.012		0.024 ± 0.012	
C19:1-Cer	0.018 ± 0.018		0.007 ± 0.005		0.030 ± 0.031		0.012 ± 0.011	
C20:1-Cer	0.024 ± 0.016		0.011 ± 0.007		0.023 ± 0.014		0.031 ± 0.014	
C21:1-Cer	0.017 ± 0.006		0.003 ± 0.003		0.016 ± 0.005		0.010 ± 0.012	
C22:1-Cer	0.249 ± 0.180		0.205 ± 0.130		0.343 ± 0.161		0.280 ± 0.078	
C23:1-Cer	0.068 ± 0.017		0.054 ± 0.016		0.148 ± 0.062		0.088 ± 0.041	

C24:1-Cer	3.295	±	1.184	2.686	±	1.200	5.821	±	2.181	3.505	±	0.848
C25:1-Cer	0.330	±	0.062	0.209	±	0.083	0.660	±	0.288	0.259	±	0.075
C26:1-Cer	0.543	±	0.057	0.451	±	0.166	1.309	±	0.680	0.554	±	0.127
C27:1-Cer	0.427	±	0.249	0.254	±	0.037	0.651	±	0.148	0.415	±	0.173
C28:1-Cer	0.212	±	0.038	0.2	±	0.056	0.479	±	0.2	0.210	±	0.057
C9:0-DhCer	0.010	±	0.003	0.006	±	0.004	0.015	±	0.013	0.012	±	0.011
C11:0-DhCer	0.006	±	0.007	0.007	±	0.004	0.015	±	0.015	0.016	±	0.009
C13:0-DhCer	0.027	±	0.014	0.012	±	0.004	0.044	±	0.031	0.024	±	0.009
C14:0-DhCer	0.021	±	0.015	0.004	±	0.004	0.051	±	0.012 ^{a*}	0.033	±	0.015
C15:0-DhCer	0.050	±	0.028	0.035	±	0.023	0.072	±	0.034	0.084	±	0.061
C16:0-DhCer	1.316	±	0.311	0.947	±	0.485	10.174	±	2.685 ^{a***}	6.706	±	2.052 ^{b*}
C17:0-DhCer	0.036	±	0.013	0.020	±	0.013	0.101	±	0.075 ^{a*}	0.080	±	0.037
C18:0-DhCer	0.110	±	0.109	0.107	±	0.043	0.672	±	0.269 ^{a***}	0.746	±	0.267
C19:0-DhCer	0.023		0.027	0.011	±	0.007	0.049	±	0.028	0.039	±	0.015
C20:0-DhCer	0.100	±	0.035	0.058	±	0.032	1.012	±	0.543 ^{a***}	0.491	±	0.227 ^{b**}
C21:0-DhCer	0.020	±	0.010	0.007	±	0.001	0.126	±	0.025	0.067	±	0.041
C22:0-DhCer	0.161	±	0.036	0.081	±	0.018	1.483	±	0.733 ^{a***}	0.733	±	0.297 ^{b***}
C23:0-DhCer	0.034	±	0.011	0.025	±	0.013	0.223	±	0.120 ^{a***}	0.109	±	0.033 ^{b***}
C24:0-DhCer	0.217	±	0.062	0.125	±	0.016	1.246	±	0.653 ^{a***}	0.577	±	0.195 ^{b***}
C25:0-DhCer	0.148	±	0.036	0.095	±	0.027	0.413	±	0.096 ^{a***}	0.173	±	0.03 ^{b***}
C26:0-DhCer	0.052	±	0.024	0.030	±	0.012	0.282	±	0.07 ^{a***}	0.098	±	0.04 ^{b***}
C27:0-DhCer	0.060	±	0.034	0.042	±	0.016	0.151	±	0.070	0.064	±	0.034
C28:0-DhCer	0.015	±	0.016	0.006	±	0.004	0.1	±	0.039 ^{a**}	0.034	±	0.010 ^{b*}
C7:1-DhCer	0.073	±	0.024	0.066	±	0.013	0.036	±	0.033	0.088	±	0.032 ^{b*}
C8:1-DhCer	0.021	±	0.016	0.006	±	0.004	0.033	±	0.035	0.010	±	0.006
C9:1-DhCer	0.012	±	0.012	0.004	±	0.004	0.041	±	0.056	0.004	±	0.005
C10:1-DhCer	0.029	±	0.014	0.012	±	0.018	0.223	±	0.419	0.01	±	0.004
C11:1-DhCer	0.015	±	0.020	0.004	±	0.005	0.012	±	0.017	0.005	±	0.002
C12:1-DhCer	0.016	±	0.0244	0.025	±	0.013	0.011	±	0.007	0.007	±	0.006
C13:1-DhCer	0.002	±	0.004	0.001	±	0.002	0.012	±	0.005 ^{a*}	0.003	±	0.003 ^{b*}
C15:1-DhCer	0.003	±	0.003	0.001	±	0.001	0.007	±	0.007	0.008	±	0.005
C16:1-DhCer	0.075	±	0.054	0.079	±	0.064	0.122	±	0.068	0.111	±	0.035
C17:1-DhCer	0.003	±	0.003	0.004	±	0.003	0.02	±	0.009 ^{a*}	0.007	±	0.005
C18:1-DhCer	0.012	±	0.002	0.017	±	0.005	0.026	±	0.014	0.037	±	0.022
C19:1-DhCer	0.014	±	0.004	0.004	±	0.007	0.038	±	0.028	0.019	±	0.015
C20:1-DhCer	0.067	±	0.069	0.010	±	0.001	0.024	±	0.004	0.013	±	0.013
C21:1-DhCer	0.004	±	0.005	0.002	±	0.002	0.003	±	0.003	0.001	±	0.002
C22:1-DhCer	0.040	±	0.023	0.016	±	0.007	0.122	±	0.062 ^{a*}	0.058	±	0.027 $^{p=0.06}$
C23:1-DhCer	0.009	±	0.012	0.008	±	0.010	0.040	±	0.013 ^{a*}	0.020	±	0.008

C24:1-DhCer	0.082	±	0.019	0.055	±	0.016	0.819	±	0.269 ^{a***}	0.485	±	0.189 ^{b**}
C25:1-DhCer	0.029	±	0.005	0.028	±	0.014	0.116	±	0.050 ^{a**}	0.067	±	0.041
C26:1-DhCer	0.027	±	0.023	0.008	±	0.004	0.179	±	0.073 ^{a***}	0.087	±	0.040 ^{b**}
C28:1-DhCer	0.014	±	0.014	0.003	±	0.004	0.087	±	0.028 ^{a***}	0.04	±	0.011 ^{b***}

Table S2. LC-ESI MS/MS analysis of N-acyl chain Cer and DhCer species distribution in zebrafish larvae of MO-control and MO-DEGS1. Experiments were performed at 5dpf +/- FTY720 (1 ng/µl) treatment. The % of individual Cer and DhCer were calculated with respect to the total Cer, DhCer respectively. Values are mean ± SD (% of total lipids analysed; n = 4) * $p<0.05$; ** $p<0.01$; *** $p<0.001$ after two-way ANOVA test followed by Tukey's posthoc test. a, indicates significant change in MO-DEGS1 from MO-control; b, indicates significant change in MO-DEGS1 after FTY720; in addition these significant correction with treatment are shadowed.

Variants	Sequence
NM_003676.3: c.397C>T	Forward: 5’- CCCAGTTGGGTGCATTTTAC -3’
	Reverse: 5’- ACCTGTGCCACGGTATTGAT -3’
NM_003676.3: 752dupT	Forward: 5’- GTGGCACAGGTCACTTTTGA -3’
	Reverse: 5’- TGAGGCATGAGAATCGTTTG -3’
NM_003676.3: c.341_342delTT	Forward: 5’- CCCAGTTGGGTGCATTTTAC -3’
	Reverse: 5’- ACCTGTGCCACGGTATTGAT -3
NM_003676.3: c.764A>G	Forward: 5’- GTGGCACAGGTCACTTTTGA -3’
	Reverse: 5’- TGAGGCATGAGAATCGTTTG -3’
NM_003676:c.604delT	Forward: 5’- AATCGCTGGTTTGGAATGT -3’
	Reverse: 5’- CAGGAATGTTGGGGAAATC -3’
NM_003676.3:c.337A>G	Forward: 5’- CCCAGTTGGGTGCATTTTAC -3’
	Reverse: 5’- ACCTGTGCCACGGTATTGAT -3’
NM_003676.3:c.320G>A	Forward: 5’- CCCAGTTGGGTGCATTTTAC -3’
	Reverse: 5’- ACCTGTGCCACGGTATTGAT -3’
NM_003676.3:c.110T>C	Forward: 5’- AGTGGGTCTACACCGACCAG -3’
	Reverse: 5’- TGGTTAATGCAACTGCCAAA -3’

Supplemental Table 3. List of primers used for Sanger validation

Full unedited gel for Supplementary Figure 4H